2010-06

Nonclassical correlation in NMR quadrupolar systems

Physical Review A,College Park : American Physical Society - APS,v. 81, n. 6, p. 062118-1-062118-9, Jun 2010
http://www.producao.usp.br/handle/BDPI/50173

Nonclassical correlation in NMR quadrupolar systems

D. O. Soares-Pinto,[1,*] L. C. Céleri,[2,†] R. Auccaise,[1] F. F. Fanchini,[3] E. R. deAzevedo,[1] J. Maziero,[2]
T. J. Bonagamba,[1] and R. M. Serra[2]

[1]*Instituto de Física de São Carlos, Universidade de São Paulo, Post Office Box 369, 13560-970 São Carlos, São Paulo, Brazil*
[2]*Centro de Ciências Naturais e Humanas, Universidade Federal do ABC, R. Santa Adélia 166, 09210-170 Santo André, São Paulo, Brazil*
[3]*Instituto de Física Gleb Wataghin, Universidade Estadual de Campinas, Post Office Box 6165, 13083-970 Campinas, São Paulo, Brazil*

(Received 31 March 2010; published 17 June 2010)

The existence of quantum correlation (as revealed by quantum discord), other than entanglement and its role in quantum-information processing (QIP), is a current subject for discussion. In particular, it has been suggested that this nonclassical correlation may provide computational speedup for some quantum algorithms. In this regard, bulk nuclear magnetic resonance (NMR) has been successfully used as a test bench for many QIP implementations, although it has also been continuously criticized for not presenting entanglement in most of the systems used so far. In this paper, we report a theoretical and experimental study on the dynamics of quantum and classical correlations in an NMR quadrupolar system. We present a method for computing the correlations from experimental NMR deviation-density matrices and show that, given the action of the nuclear-spin environment, the relaxation produces a monotonic time decay in the correlations. Although the experimental realizations were performed in a specific quadrupolar system, the main results presented here can be applied to whichever system uses a deviation-density matrix formalism.

DOI: 10.1103/PhysRevA.81.062118 PACS number(s): 03.65.Ud, 03.67.Mn, 03.67.Lx, 76.60.−k

I. INTRODUCTION

Since the birth of quantum-information theory (QIT), entanglement has been considered as a key resource for the processing of information at a quantum level. However, it is known that quantum correlation may be present even in separable states. This nonclassical correlation can be quantified, for example, by the so-called quantum discord [1], which is a measure of a gap between quantum- and classical-information theory. Some other measures for both classical and quantum correlations contained in a bipartite quantum state were proposed in literature [2–9]. Nonclassical correlation may exist in almost all quantum states [10], and it has been theoretically [11] and experimentally [12] demonstrated that it may provide computational speedup in a model of quantum computation. Also, it was suggested [13] that the speedup of some quantum algorithms may be due to quantum correlation of separable states.

The study of the nonclassical aspects of a correlated quantum system, especially the aspect revealed by quantum discord, received a great deal of attention in recent scientific literature [11,14–27]. In particular, the action of decoherence on this correlation was studied by taking different kinds of environmental interactions [15,23–25,28] into account. Until now, only two experimental measurements of such a nonclassical correlation have been performed [12,29]. In Ref. [12], by means of an optical architecture, the authors implemented the so-called deterministic quantum computation with one qubit [30] for the trace estimation of a unitary matrix. In such a nonuniversal quantum-information-processing (QIP) model, entanglement is not a necessary resource for obtaining a computational speedup (in comparison with the best classical algorithm). The authors of Ref. [29] demonstrated, also using an optical setup, the sudden change in the decay rates of classical and quantum correlations, theoretically predicted in Ref. [15].

Nuclear magnetic resonance (NMR) systems have been extensively used as a method for implementing and benching test QIP ideas [31,32]. The main feature of the technique is the excellent control of unitary transformations provided by the use of radio-frequency (rf) pulses, which result in unique methods for quantum-state manipulation [33,34] and generation of protocols for processing quantum information [31,35,36]. For example, algorithms such as Deutsch-Jozsa, Shor, and Grover were successfully tested using NMR systems [31,32]. However, most of these achievements were performed in bulk samples (bulk NMR) by using the so-called pseudopure states, for which the existence of entanglement was promptly ruled out [37–39]. This last fact has led to the questioning of the quantum nature of NMR implementations for QIP. On the other hand, as suggested in Refs. [13,37], the existence of quantum correlation, other than entanglement in NMR systems, may be the reason for the success of most bulk NMR implementations. Moreover, as mentioned before, quantum correlation of separable states may provide computational speedup in some tasks.

To our knowledge, here, we present the first demonstration that both quantum and classical correlations in NMR systems can be determined from experimentally detectable deviation-density matrices. We use an NMR quadrupolar system to theoretically and experimentally study the existence of quantum and classical correlations in a two-logical-qubit composite system. Our results show that such a nonclassical correlation can easily be created and can be manipulated at room temperature. We also investigate how these correlations are degraded by the effect of the environment on the nuclear spin. In our system, the quantum aspect of correlation decays monotonically within the relaxation time of the deviation matrix. Our experimental implementations were carried out by using an effective two-qubit representation of an ^{23}Na nuclear

*diogo.osp@ursa.ifsc.usp.br
†lucas.celeri@ufabc.edu.br

spin ($I = 3/2$) in a lyotropic liquid-crystal [sodium dodecyl sulfate (SDS)] sample at 26°C. The achievements presented here, together with the discussion about the role of quantum correlation (of separable states) in QIP, reinforce the relevance of the NMR tools in this scenario.

This paper is organized as follows. In Sec. II, we briefly review the description of the NMR quadrupolar system. Section III is devoted to presenting the method for determining the quantum and classical correlations from the experimentally accessible NMR deviation-density matrix. Also in this section, we present a theoretical model to describe the relaxation dynamics in our system. The experimental results are presented in Sec. IV; and, in Sec. V, we present a summary and a discussion.

II. DESCRIPTION OF THE SYSTEM

In NMR systems, at room temperature, the energy gaps between the levels of the system $\delta E = \hbar\omega_L$ are much smaller than the thermal energy $\epsilon = \hbar\omega_L/2k_BT \sim 10^{-5}$ (we added, for convenience, a $1/2$ factor in the definition of ϵ). This implies that a typical NMR-system density matrix can be written, in the high-temperature expansion [31,40], as

$$\rho \approx \frac{1}{Z}\mathbf{1} + \epsilon\Delta\rho, \tag{1}$$

where $\mathbf{1}$ is the $2^n \times 2^n$ identity matrix, with n being the number of effective logical qubits in the QIP terminology, $Z \approx 2^n$ is the system-partition function [31], and $\Delta\rho$ is the traceless deviation-density matrix. In general, the state described in Eq. (1) is a mixed state that does not possess entanglement [38,39]. However, as we will show in what follows, it might have quantum correlation (of separable states) that can be used in QIP protocols [11,12].

Any manipulation—such as state preparation, state tomography, qubit rotations, and so on—is performed only onto the deviation matrix $\Delta\rho$. For example, a sequence of rf pulses, which can be represented by a unitary transformation U, changes the density operator in the following way:

$$U\rho U^\dagger = \frac{1}{2^n}\mathbf{1} + \epsilon U\Delta\rho U^\dagger. \tag{2}$$

By a suitable adjustment of each rf pulse length, phase, and amplitude, very fine control over the density-matrix populations and coherences (diagonal and off-diagonal elements, respectively) can be achieved. Together with proper temporal or spatial averaging procedures [41] and evolution under spin interactions, the rf pulse can be specially designed to prepare the system in all two-qubit computational base states as well as its superpositions, starting from the thermal-equilibrium state (Boltzmann distribution) [42,43]. The effect of the environment on the spin system is to induce relaxation in such a way that, after characteristic times, the populations return to the equilibrium distribution and the coherences vanish.

The purpose of this paper is to theoretically and experimentally investigate the presence of quantum and classical correlations and their degradation due to decoherence for different initial states of a two-qubit representation of the nuclear-spin system. To achieve this goal, we use a spin $I = 3/2$ quadrupolar NMR system. In the presence of a static magnetic field, due to the Zeeman splitting, nuclei with $I > 1/2$ can be described by a $(2I + 1)$-level system with equally spaced energy levels. However, such nuclei also possess quadrupole moments, which interact with the electric-field gradient (EFG) produced by the charge distribution in their surroundings, the so-called quadrupolar interaction [31]. When the Zeeman interaction is much stronger than the quadrupolar one, the latter can be treated in the framework of first-order perturbation theory, and the system's Hamiltonian turns out to be [44–46]

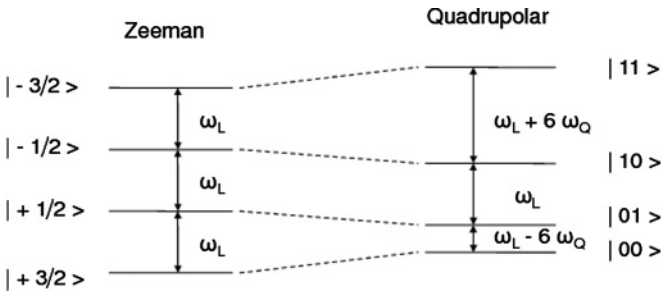

FIG. 1. Sketch of the four energy levels in the spin $I = 3/2$ system (characterized by the z component of the nuclear-spin magnetization) for the Zeeman and the quadrupolar couplings. The indexation of the effective two-qubit computational basis is also displayed.

$$\mathcal{H} = -\hbar\omega_L I_z + \hbar\omega_Q\left(3I_z^2 - \mathbf{I}^2\right), \tag{3}$$

where ω_L and ω_Q are the Larmor and the quadrupole frequencies, respectively ($|\omega_L| \gg |\omega_Q|$). The spin-nuclear operator is characterized by its z component I_z and its square modulus $\mathbf{I}^2$. The first term of Eq. (3) describes the Zeeman interaction while the second one accounts for the static first-order quadrupolar interaction [44–46].

This system can be regarded as an effective two-qubit quantum system that may be used for QIP [31,32,35,41,47]. Figure 1 shows a sketch of the four energy levels in the case $I = 3/2$, characterized by the z component of the nuclear-spin magnetization whose projections are $m = -3/2, -1/2, 1/2, 3/2$. Figure 1 also displays the logical indexing of the angular momentum basis [i.e., the computational basis (for the effective two-qubit system)] as well as the three single quantum transitions that can be directly detected after applying a nonselective $\pi/2$ rf pulse onto the system (equilibrium spectrum). Although the implementation of the qubit in a quadrupolar system, as considered here, is not so obvious, many experiments proved that logic gates as well as quantum algorithms can be realized in such an effective system [48,49].

III. QUANTUM AND CLASSICAL CORRELATIONS AND THEIR DYNAMICS UNDER DECOHERENCE

Let us now briefly review two proposed measures to quantify the quantum and classical aspects of the correlation contained in a bipartite quantum system. The nonclassical correlation in a composed state can be quantified by quantum discord [1], and its classical counterpart is given by the Henderson-Vedral measure [2,3]. In what follows, we will also discuss a measure of quantum correlation that can be

regarded as a symmetrical version of quantum discord [25,26] and its classical counterpart [8,9]. A suitable expansion of the correlation measures, in terms of the experimental measurable deviation matrix [cf. Eq. (1)], will then be obtained. Finally, we present the dynamic equations governing the evolution of the density operator of a spin $I = 3/2$ system under the action of a typical spin environment in an NMR quadrupolar scenario, using the Redfield formalism [50,51].

A. Measures of correlations

The mutual information is a measure of the correlation between two random variables A and B in classical information theory [52],

$$I_c(A{:}B) = \mathcal{H}(A) + \mathcal{H}(B) - \mathcal{H}(A,B), \tag{4}$$

where $\mathcal{H}(X) = -\sum_x p_x \log_2 p_x$ is the Shannon entropy of the variable X with p_x being the probability of variable X assuming the value x. By means of the Bayes rule, we can rewrite Eq. (4) in an equivalent form

$$J_c(A{:}B) = \mathcal{H}(A) - \mathcal{H}(A|B), \tag{5}$$

with $\mathcal{H}(A|B) = -\sum_{a,b} p_{a,b} \log_2 p_{a|b}$ $(p_{a|b} = p_{a,b}/p_b)$ being the conditional entropy, which represents the lack of knowledge of variable A when we know (by means of a measurement) the value of variable B. It is clear that, in the classical case, we always have $I_c(A{:}B) - J_c(A{:}B) = 0$.

In the realm of QIT, while the extension of Eq. (4) for a bipartite quantum state (ρ_{AB}) is trivially obtained as [53–55]

$$\mathcal{I}(\rho_{A:B}) = S(\rho_A) + S(\rho_B) - S(\rho_{AB}), \tag{6}$$

the extension of Eq. (5) is not so straightforward. Here, $S(\rho) = -\mathrm{Tr}(\rho \log_2 \rho)$ is the von Neumann entropy, and $\rho_{A(B)} = \mathrm{Tr}_{B(A)}(\rho_{AB})$ is the reduced-density operator of partition $A(B)$. The quantum mutual information given in Eq. (6) is a measure of the total correlation (including the classical and the quantum ones) contained in a bipartite quantum system [5,56]. The quantum extensions of Eqs. (4) and (5) are not equivalent, in general; and this inequivalence relies on the distinct nature of both quantum and classical measurements. While the classical measurement can be chosen such that it does not disturb the system to be measured in the quantum case, the measurement process may affect the system in a fundamental manner. This observation leads Ollivier and Zurek [1] to propose a measure of quantum correlation, named quantum discord, given by the difference,

$$\mathcal{D}(\rho_{AB}) \equiv \mathcal{I}(\rho_{A:B}) - \max_{\{\Pi_j^B\}} \mathcal{J}(\rho_{A:B}), \tag{7}$$

where $\mathcal{J}(\rho_{A:B}) = S(\rho_A) - S_{\{\Pi_j^B\}}(\rho_{A|B})$, with $S_{\{\Pi_j^B\}}(\rho_{A|B}) = \sum_j q_j S(\rho_A^j)$ being a quantum extension of the classical conditional entropy $\mathcal{H}(A|B)$. The reduced state of partition A (ρ_A^j), after the measurement Π_j^B is performed on partition B, is given by $\rho_A^j = \mathrm{Tr}_B\{(\mathbf{1}_A \otimes \Pi_j^B)\rho_{AB}(\mathbf{1}_A \otimes \Pi_j^B)\}/q_j$, with $q_j = \mathrm{Tr}_{AB}[(\mathbf{1}_A \otimes \Pi_j^B)\rho_{AB}]$ ($\mathbf{1}_A$ is the identity operator for partition A). The quantum discord Eq. (7) is computed by an extremization procedure over all possible complete sets of projective measurements $\{\Pi_j^B\}$ over subsystem B.

Due to the distinct nature of quantum and classical correlations, we can assume that both correlations add up in a simple way to give the quantum mutual information. Therefore, the classical counterpart of the quantum discord may be defined simply as [15,25]

$$\mathcal{C}(\rho_{AB}) \equiv \mathcal{I}(\rho_{A:B}) - \mathcal{D}(\rho_{AB}), \tag{8}$$

that is identical to the Henderson-Vedral definition of classical correlation [2,3].

In some circumstances, the quantum discord, Eq. (7), and its classical counterpart, Eq. (8), may be asymmetric with respect to the choice of the partition to be measured (see Refs. [25,26] for a related discussion concerning symmetric measures of correlations). Since the states considered in this paper are, in general, asymmetric by an interchange between the two partitions, we will use symmetrized versions for the measures of both quantum and classical correlations. Alternatively, the classical correlation in a composite bipartite system can be expressed as the maximum classical mutual information that is obtained by local measurements over both partitions of a composite state [8,9],

$$\mathcal{K}(\rho_{AB}) \equiv \max_{\{\Pi_i^A \otimes \Pi_j^B\}} [I_c(A{:}B)], \tag{9}$$

where $I_c(A{:}B)$ is the classical mutual information defined in Eq. (4) for the probability distributions that result from the quantum-measurement process. The extremization in Eq. (9) is taken over the set of local projective measurements $\{\Pi_i^A \otimes \Pi_j^B\}$ over both subsystems. Since the quantum mutual information quantifies the total correlation, a symmetrized measure of the quantum correlation can be defined as [25,26]

$$\mathcal{Q}(\rho_{AB}) \equiv \mathcal{I}(\rho_{A:B}) - \mathcal{K}(\rho_{AB}). \tag{10}$$

For composite states of two qubits with maximally mixed marginals, the quantum discord Eq. (7) is identical to its symmetrized version Eq. (10) (i.e., $\mathcal{D}(\rho_{AB}) = \mathcal{Q}(\rho_{AB})$ [and also $\mathcal{K}(\rho_{AB}) = \mathcal{C}(\rho_{AB})$]). However, it is not true in general [25,26]. We can regard Eq. (10) as a symmetrical version of quantum discord. Indeed, such a symmetrical quantifier also reveals a departure between the quantum and the classical versions of information theory.

B. Correlations and the deviation matrix

For our purposes, the initial NMR density matrix can be written in terms of the deviation matrix as

$$\rho = \tfrac{1}{4} + \epsilon \Delta\rho. \tag{11}$$

The deviation matrix $\Delta\rho$ can be experimentally reconstructed using a set of rf pulses and readouts [quantum-state tomography (QST)] [31,32]. The parameter ϵ may be estimated from the Zeeman and thermal-energy ratios (in our experiment, at room temperature, $\epsilon \ll 1$). Since all correlations present in the state ρ come from the deviation matrix $\Delta\rho$, it is convenient to express the measures of correlations as functions of $\Delta\rho$. To do this, we will expand the von Neumann entropy in powers of the small parameter ϵ as follows:

$$S(\rho) = 2\left(1 - \frac{\epsilon^2}{\ln 2}\mathrm{Tr}\Delta\rho^2\right) + \cdots, \tag{12}$$

where we used the fact that $\mathrm{Tr}\Delta\rho = 0$. The reduced-density operator reads $\rho_{A(B)} = \mathrm{Tr}_{B(A)}\rho = \mathbf{1}_{A(B)}/2 + \epsilon\Delta\rho_{A(B)}$, with $\Delta\rho_{A(B)} = \mathrm{Tr}_{B(A)}\Delta\rho$. We observe that because $\mathrm{Tr}\Delta\rho = 0$, we have $\mathrm{Tr}\Delta\rho_A = \mathrm{Tr}\Delta\rho_B = 0$. Thus, the marginal entropies are straightforwardly obtained as

$$S(\rho_{A(B)}) = 1 - \frac{\epsilon^2}{\ln 2}\mathrm{Tr}\Delta\rho_{A(B)}^2 + \cdots. \tag{13}$$

By replacing Eqs. (12) and (13) into Eq. (6) and by disregarding terms containing high powers in ϵ, we obtain

$$\mathcal{I}(\rho) \approx \frac{\epsilon^2}{\ln 2}\left(2\mathrm{Tr}\Delta\rho^2 - \mathrm{Tr}\Delta\rho_A^2 - \mathrm{Tr}\Delta\rho_B^2\right). \tag{14}$$

To compute the classical correlation, we must obtain the measured density operator, which is given by

$$\begin{aligned}\eta &= \sum_{i,j}\left(\Pi_i^A \otimes \Pi_j^B\right)\rho\left(\Pi_i^A \otimes \Pi_j^B\right)\\ &\equiv \frac{\mathbf{1}}{4} + \epsilon\Delta\eta,\end{aligned} \tag{15}$$

where we defined the measured deviation matrix as $\Delta\eta \equiv \sum_{i,j}(\Pi_i^A \otimes \Pi_j^B)\Delta\rho(\Pi_i^A \otimes \Pi_j^B)$. For a two-qubit system, the complete set of projective measurements is given by $\{\Pi_j^k = |\Theta_j^k\rangle\langle\Theta_j^k|, j = \|, \perp, k = A,B\}$, where $|\Theta_\|^k\rangle \equiv \cos(\theta_k)|0_k\rangle + e^{i\phi_k}\sin(\theta_k)|1_k\rangle$ and $|\Theta_\perp^k\rangle \equiv e^{-i\phi_k}\sin(\theta_k)|0_k\rangle - \cos(\theta_k)|1_k\rangle$ with $0 \leqslant \theta_k \leqslant \pi$ and $0 \leqslant \phi_k \leqslant 2\pi$. $\{|0_k\rangle,|1_k\rangle\}$ is the computational basis of the logical qubit of partition k. We note that the correlation quantifiers, presented here, have the same values for simultaneous or successive measurements performed on each partition.

The same reasoning that results in Eq. (14) leads us to the following expression, in terms of the measured deviation matrix, for the mutual information of the measured state,

$$I_c(\eta) \approx \frac{\epsilon^2}{\ln 2}[2\mathrm{Tr}\Delta\eta^2 - \mathrm{Tr}(\Delta\eta_A)^2 - \mathrm{Tr}(\Delta\eta_B)^2]; \tag{16}$$

and, thus, for the classical correlation,

$$\mathcal{K}(\rho) \approx \max_{\{\Pi_i^A \otimes \Pi_j^B\}} I_c(\eta), \tag{17}$$

where $\Delta\eta_{A(B)} = \mathrm{Tr}_{B(A)}\Delta\eta$ is the reduced measured deviation matrix of partition $A(B)$. The quantum correlation in the composed two-qubit system can be directly computed from Eqs. (14) and (17) as $\mathcal{Q}(\rho) = \mathcal{I}(\rho) - \mathcal{K}(\rho)$.

C. Action of the environment on the deviation matrix

As commented on Sec. II, the quadrupolar coupling emerges from the interaction of the nuclear quadrupole moment with the EFG generated by the surrounding environment. Internal molecular or atomic motions cause random fluctuations in the EFG, which introduces noise into the system, which leads to the relaxation process that causes decoherence and energy dissipation. The dependence of the random EFG fluctuations on the molecular motions is established by the spectral densities that encode the motion characteristics, such as geometry and correlation times [57].

Our experimental implementations were carried out using ^{23}Na nuclear spins ($I = 3/2$) in a lyotropic liquid crystal at 26°C. In this system, the relaxation of the ^{23}Na nuclear spin can be well described by considering a pure quadrupolar mechanism (the relaxation is produced exclusively by the EFG fluctuations), so it can be represented by three reduced spectral densities J_0, J_1, and J_2 at the Larmor frequency ω_L. The specific model that relates the molecular motions and the reduced spectral densities can be found in Ref. [59]. By applying the Redfield formalism [51] to our system, enables us to obtain the dynamic evolution of the deviation-density matrix elements $\Delta\rho_{ij}$ (i,j running from 0 to 3) as [59]

$$\begin{aligned}\Delta\rho_{01}(t) &= \tfrac{1}{2}\left[\Delta\rho_{01}^0 + \Delta\rho_{23}^0\right.\\ &\quad\left.+ \left(\Delta\rho_{01}^0 - \Delta\rho_{23}^0\right)e^{-2CJ_2t}\right]e^{-C(J_0+J_1)t},\end{aligned} \tag{18a}$$

$$\begin{aligned}\Delta\rho_{02}(t) &= \tfrac{1}{2}\left[\Delta\rho_{02}^0 + \Delta\rho_{13}^0\right.\\ &\quad\left.+ \left(\Delta\rho_{02}^0 - \Delta\rho_{13}^0\right)e^{-2CJ_1t}\right]e^{-C(J_0+J_2)t},\end{aligned} \tag{18b}$$

$$\begin{aligned}\Delta\rho_{13}(t) &= \tfrac{1}{2}\left[\Delta\rho_{02}^0 + \Delta\rho_{13}^0\right.\\ &\quad\left.- \left(\Delta\rho_{02}^0 - \Delta\rho_{13}^0\right)e^{-2CJ_1t}\right]e^{-C(J_0+J_2)t},\end{aligned} \tag{18c}$$

$$\begin{aligned}\Delta\rho_{23}(t) &= \tfrac{1}{2}\left[\Delta\rho_{01}^0 + \Delta\rho_{23}^0\right.\\ &\quad\left.- \left(\Delta\rho_{01}^0 - \Delta\rho_{23}^0\right)e^{-2CJ_2t}\right]e^{-C(J_0+J_1)t},\end{aligned} \tag{18d}$$

$$\Delta\rho_{03}(t) = \Delta\rho_{03}^0 e^{-C(J_1+J_2)t}, \tag{18e}$$

$$\Delta\rho_{12}(t) = \Delta\rho_{12}^0 e^{-C(J_1+J_2)t}, \tag{18f}$$

$$\begin{aligned}\Delta\rho_{00}(t) &= 3 - \tfrac{1}{4}[R_1 e^{-2C(J_1+J_2)t}.\\ &\quad - R_2 e^{-2CJ_2t} - R_3 e^{-2CJ_1t}],\end{aligned} \tag{18g}$$

$$\begin{aligned}\Delta\rho_{11}(t) &= 1 + \tfrac{1}{4}[R_1 e^{-2C(J_1+J_2)t}\\ &\quad + R_2 e^{-2CJ_2t} - R_3 e^{-2CJ_1t}],\end{aligned} \tag{18h}$$

$$\begin{aligned}\Delta\rho_{22}(t) &= -1 + \tfrac{1}{4}[R_1 e^{-2C(J_1+J_2)t}\\ &\quad - R_2 e^{-2CJ_2t} + R_3 e^{-2CJ_1t}],\end{aligned} \tag{18i}$$

$$\begin{aligned}\Delta\rho_{33}(t) &= -3 - \tfrac{1}{4}[R_1 e^{-2C(J_1+J_2)t}\\ &\quad + R_2 e^{-2CJ_2t} + R_3 e^{-2CJ_1t}].\end{aligned} \tag{18j}$$

In Eqs. (18a)–(18j), the superscript 0 refers to the initial value of each deviation-matrix element and R_i ($i = 1,2,3$) are constant coefficients. The labels of the deviation-matrix elements $\{0,1,2,3\}$ refer to the computational basis of the effective two-qubit system ordered in the usual way $\{|00\rangle,|01\rangle,|10\rangle,|11\rangle\}$. The parameter C is proportional to the quadrupolar coupling ω_Q and can be obtained from the equilibrium NMR spectrum (displayed in Fig. 2) [58,59]. To fully describe the system relaxation, it is also necessary to determine the spectral densities J_i ($i = 0,1,2$) as well as the coefficients R_j ($j = 1,2,3$). This can be achieved by preparing an initial state by using the technique of strongly modulated pulses (SMPs) [60–62], together with temporal averaging, where all $\Delta\rho$ coherences are nonzero (the full superposition state), by letting it evolve under the action of relaxation during a time period τ, and then by measuring each $\Delta\rho$ element using QST [62]. By repeating this procedure for different values of τ, the relaxation dynamics for each $\Delta\rho$ element is experimentally measured. In Fig. 3, we depict the pulse-sequence scheme of the experimental procedure used. We note that Eqs. (18a)–(18j) are valid for whichever initial state of the system, with the asymptotic state being the equilibrium one, $\rho = \mathbf{1}/4 + \epsilon 2I_Z$.

Equations (18a)–(18j) can be combined to provide single-exponential functions in the following way [59]:

$$\Delta\rho_{01} + \Delta\rho_{23} = \left(\Delta\rho_{01}^0 + \Delta\rho_{23}^0\right)e^{-C(J_0+J_1)t}, \tag{19a}$$

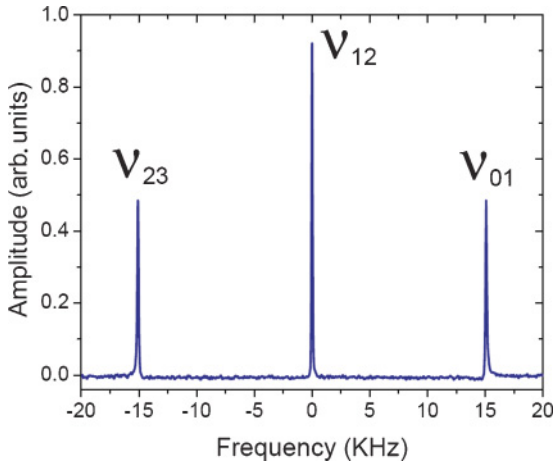

FIG. 2. (Color online) ^{23}Na NMR equilibrium spectrum of the oriented liquid-crystal SDS sample. The frequencies ν_{01}, ν_{12}, and ν_{23} correspond to the transitions $|00\rangle \leftrightarrow |01\rangle$, $|01\rangle \leftrightarrow |10\rangle$, and $|10\rangle \leftrightarrow |11\rangle$, respectively.

$$\Delta\rho_{02} - \Delta\rho_{13} = \left(\Delta\rho_{02}^{0} + \Delta\rho_{13}^{0}\right)e^{-C(J_0+J_2)t}, \tag{19b}$$

$$\Delta\rho_{12} = \Delta\rho_{12}^{0}e^{-C(J_1+J_2)t}, \tag{19c}$$

$$\Delta\rho_{00} + \Delta\rho_{11} - \Delta\rho_{22} - \Delta\rho_{33} = 8 + R_2e^{-2CJ_2t}, \tag{19d}$$

$$-\Delta\rho_{00} + \Delta\rho_{11} + \Delta\rho_{22} - \Delta\rho_{33} = R_1e^{-2C(J_1+J_2)t}, \tag{19e}$$

$$\Delta\rho_{00} - \Delta\rho_{11} + \Delta\rho_{22} - \Delta\rho_{33} = 4 + R_3e^{-2CJ_1t}. \tag{19f}$$

For convenience, in Eqs. (19a)–(19f), we have suppressed the temporal dependence of the deviation-matrix elements $\Delta\rho_{ij}(t)$. Thus, by fitting the experimental evolution of the deviation-matrix elements, it is possible to determine the mean values of the reduced spectral densities J_i by using Eqs. (19a)–(19c) and to determine the parameters R_j by using Eqs. (19d)–(19f). We also checked the consistency of the experimental data with the adopted relaxation model by comparing the values of J_1 and J_2 obtained from Eqs. (19a)–(19c) and Eqs. (19d)–(19f) (see Ref. [59] for specific details).

The relaxation dynamics of the system can also be described by the time dependence of the mean value of I_z and $I_{x,y}$

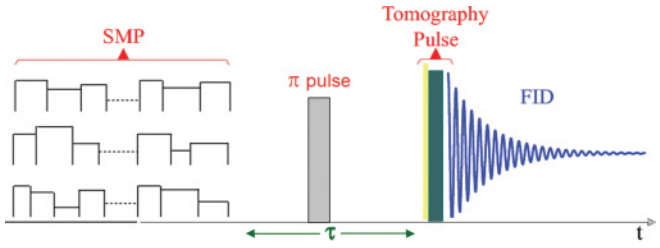

FIG. 3. (Color online) Scheme of the pulse sequence used in the experimental procedure. The first step is the state preparation through a sequence of SMPs [60]. Next, we leave the system to evolve only under the action of the decoherent environment during a variable period of time τ. The last step is the nonselective tomography pulse and the observation of the free induction decay (FID) signal, which enable us to reconstruct the deviation-density matrix $\Delta\rho$ through QST [62]. The π pulse was added in the middle of the free evolution period to refocus the B_0-field inhomogeneities.

[$\langle I_z\rangle(t)$—longitudinal relaxation, $\langle I_{x,y}\rangle(t)$—transverse relaxation], which can be calculated by using Eqs. (18a)–(18j) as

$$\begin{aligned}\langle I_z\rangle(t) - \langle I_z\rangle_T &= \tfrac{1}{2}\{3\Delta\rho_{00} + \Delta\rho_{11} - \Delta\rho_{22} - 3\Delta\rho_{33}\} - 5 \\ &= 5 + \tfrac{1}{2}\{2R_2e^{-2CJ_2t} + R_3e^{-2CJ_1t}\},\end{aligned} \tag{20}$$

and

$$\begin{aligned}\langle I_x\rangle(t) + i\langle I_y\rangle(t) &= 2\Delta\rho_{21} \\ &= \Delta\rho_{21}^{0}e^{-C(J_1+J_2)t}.\end{aligned} \tag{21}$$

In Eq. (20), $\langle I_z\rangle_T$ represents $\langle I_z\rangle$ for the thermal-equilibrium state. The longitudinal relaxation is then characterized by the time constants $\tau_{L_1} = (2CJ_1)^{-1}$ and $\tau_{L_2} = (2CJ_2)^{-1}$, and the transverse relaxation is characterized by the time constant $\tau_T = [C(J_1 + J_2)]^{-1}$ [63,64].

It is important to note that, in our effective two-qubit representation of the four-level system, the environment acts globally (i.e., it acts simultaneously on both logical qubits). Such global action of the environment can be observed in the form of Eqs. (18a)–(18j), where we do not have distinct spectral densities for each qubit. We recall that we can consider this $I = 3/2$ system as an effective two-qubit one since we can manipulate the transitions between the energy levels of these logical qubits (i.e., the nuclear transitions of the quadrupolar spin) just as it is performed in the case of physical qubits [43].

IV. EXPERIMENTAL RESULTS

In our experiment, the sample of ^{23}Na nuclei, in a lyotropic liquid crystal, was prepared with 20.9 wt% of SDS (95% of purity), 3.7 wt% of decanol, and 75.4 wt% of deuterium oxide, by following the procedure described in Ref. [65]. The ^{23}Na NMR experiments were performed in a 9.4-T–VARIAN INOVA spectrometer using a 7-mm solid-state NMR probe head at $T = 26^{\circ}$C. Figure 2 shows the equilibrium spectrum for our sample. From this spectrum, we obtained the quadrupole frequency $\nu_Q = 6\omega_Q/2\pi = 15$ kHz and the constant parameter $C = (12 \pm 1) \times 10^9$ s^{-2}. By following the procedure described in Sec. III C, we estimated the values of the spectral densities as $J_0 = (17 \pm 4) \times 10^{-9}$ s, $J_1 = (3.0 \pm 0.5) \times 10^{-9}$ s, and $J_2 = (3.4 \pm 0.5) \times 10^{-9}$ s. Consequently, the time constants that appear in Eqs. (20) and (21) are $\tau_{L_1} = (13 \pm 4)$ ms, $\tau_{L_2} = (14 \pm 4)$ ms, and $\tau_T = (13 \pm 4)$ ms. Finally, the mean values obtained for the constant parameters R_j are $R_1 = -1.9 \pm 0.2$, $R_2 = -7.9 \pm 0.1$, and $R_3 = -4.5 \pm 0.2$.

By means of numerically optimized rf pulses (SMP technique) [60–62] and temporal averaging, we prepared the deviation-density matrices, which correspond to five distinct initial states: an arbitrary random X-type pseudopure state ($|X_{\text{random}}\rangle$) and the four Bell-basis pseudopure states $\{|\Psi^{\pm}\rangle = (|00\rangle \pm |11\rangle)/\sqrt{2}, |\Phi^{\pm}\rangle = (|01\rangle \pm |10\rangle)/\sqrt{2}\}$. All of these initial pseudopure states have the following form, in the computational basis, for the corresponding deviation

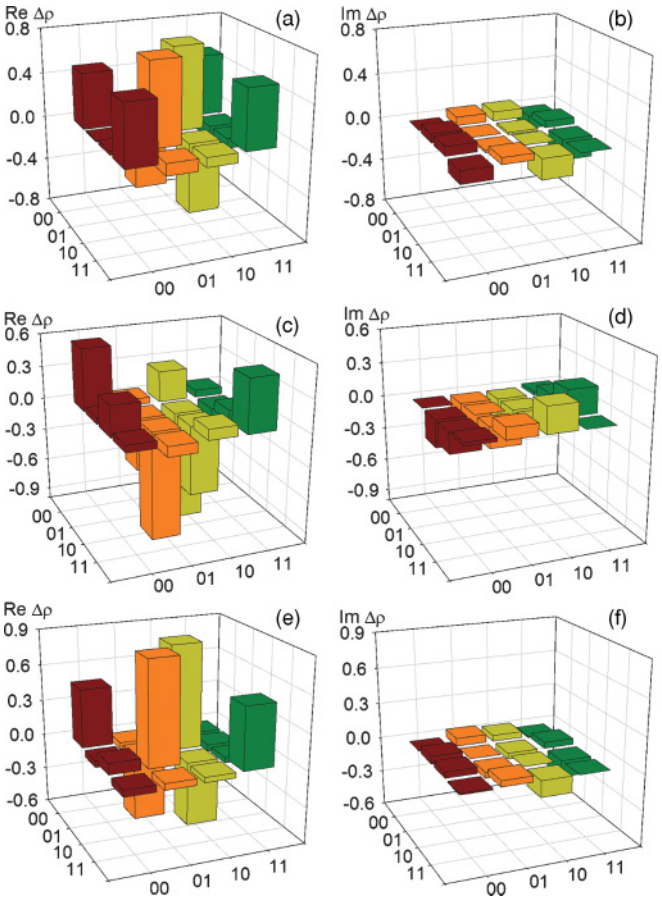

FIG. 4. (Color online) Bar representation of the QST experimental data for the prepared deviation matrix: (a) real and (b) imaginary parts of the equivalent to $|X_{\text{random}}\rangle$ pseudopure state; (c) real and (d) imaginary parts of the equivalent to $|\Phi^-\rangle$ Bell-basis pseudopure state; (e) real and (f) imaginary parts of the equivalent to $|\Phi^+\rangle$ Bell-basis pseudopure state.

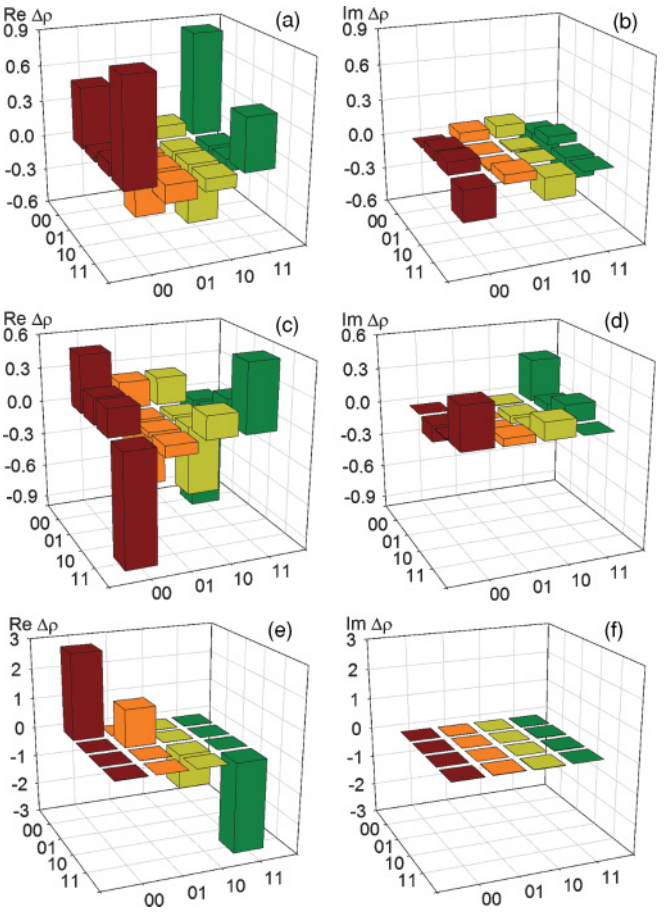

FIG. 5. (Color online) Bar representation of the QST experimental data for the prepared deviation matrix: (a) real and (b) imaginary parts of the equivalent to $|\Psi^+\rangle$ Bell-basis pseudopure state; (c) real and (d) imaginary parts of the equivalent to $|\Psi^-\rangle$ Bell-basis pseudopure state; (e) real and (f) imaginary parts of the equilibrium state.

matrices,[1]

$$\Delta\rho_R = \begin{bmatrix} a & 0 & 0 & f \\ 0 & b & e & 0 \\ 0 & e^* & c & 0 \\ f^* & 0 & 0 & d \end{bmatrix}. \tag{22}$$

The five prepared initial-state deviation matrices are displayed as a bar representation in Figs. 4(a)–4(f) and Figs. 5(a)–5(d).The mean fidelity of the *prepared* states relative to the *ideal* ones is $\mathcal{F} = (\sqrt{\rho_{\text{ideal}}}\rho_{\text{prepared}}\sqrt{\rho_{\text{ideal}}})^{1/2} \approx 0.98$. We note that, independent of the initial state considered, the asymptotic state is always given by the thermal equilibrium state whose deviation matrix is $\Delta\rho = 2I_z$ [displayed in Figs. 5(e) and 5(f)].

The reconstruction of the deviation-density matrix was performed through QST described in Ref. [62]. The relaxation dynamics of the elements was followed using the procedure described in Sec. III C. We computed the quantum correlation and its classical counterpart present in the effective two-qubit pseudopure state accordingly in Sec. III B [i.e., they were computed through Eqs. (10), (14), and (17) by using the experimental reconstructed deviation matrix for different evolution periods $\tau = n\Delta\tau$ ($n = 1, \ldots, 40$). For each initial state, the free evolution depicted in the pulse sequence displayed in Fig. 3 was performed 40 times with an evolution-period increment of $\Delta\tau = 1.5$ ms, leading to a maximum evolution time of 60 ms. The errors bars in Figs. 6(a)–6(c) and Figs. 7(a) and 7(b) were estimated from the standard deviation of three or more realizations of the whole experimental procedure (sketched in Fig. 3) for each initial state (prepared via the SMP technique).

We display the decoherence dynamics of correlations (classical, quantum, and the mutual information) present in the two-qubit pseudopure states corresponding to $|X_{\text{random}}\rangle$, $|\Psi^+\rangle$, $|\Psi^-\rangle$, $|\Phi^+\rangle$, and $|\Phi^-\rangle$ in Figs. 6(a)–6(c), 7(a), and 7(b), respectively. The theoretical curves obtained from the model presented in Sec. III C are in very good agreement with the experimental data. In these figures, we observe that the correlations decay monotonically (as an exponential law) under the action of the nuclear-spin environment. We also note that for the Bell-basis pseudopure states [$|\Psi^\pm\rangle$,$|\Phi^\pm\rangle$, Figs. 6(b) and 6(c) and Figs. 7(a) and 7(b)], the quantum

[1] In our experiment, the null elements of the deviation-density matrix are zero within the experimental errors.

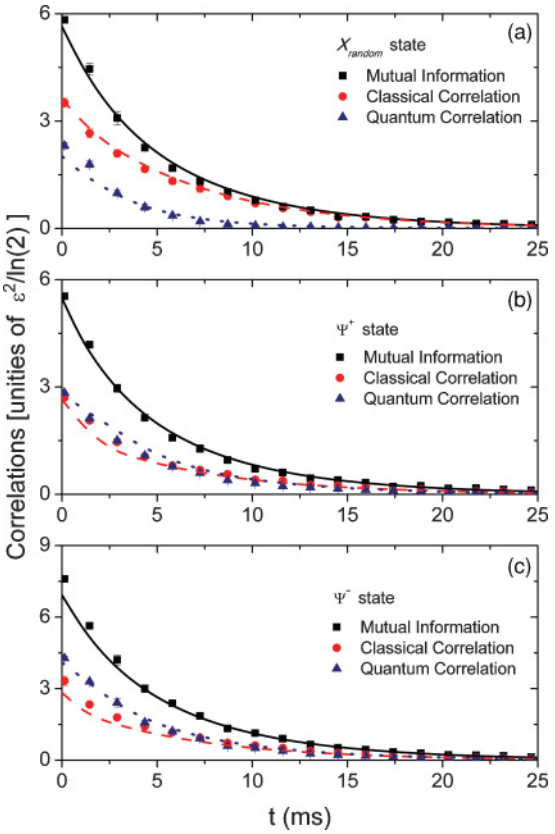

FIG. 6. (Color online) Correlations in the effective two-qubit pseudopure states. The solid lines represent the theoretical model, and the marks are the experimental points.

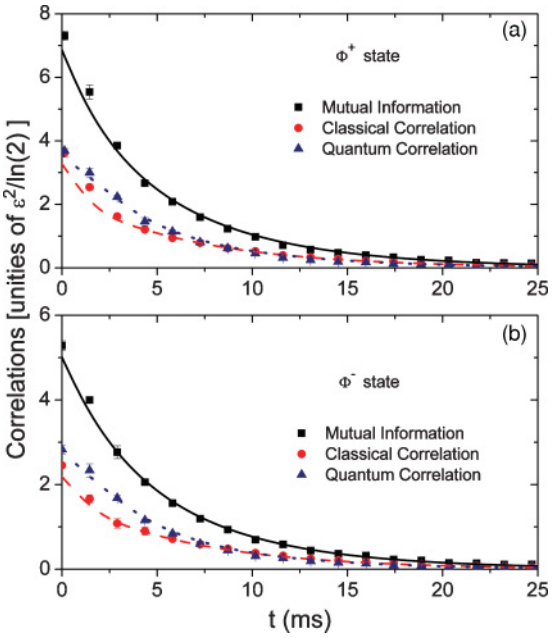

FIG. 7. (Color online) Correlations in the effective two-qubit pseudopure states. The solid lines represent the theoretical model, and the marks are the experimental points.

correlation is typically greater than its classical counterpart $\mathcal{Q}(\rho_{AB}) \geqslant \mathcal{K}(\rho_{AB})$. The opposite situation occurs for the chosen $|X_{\text{random}}\rangle$ pseudopure state [Fig. 6(a)] where $\mathcal{Q}(\rho_{AB}) \leqslant \mathcal{K}(\rho_{AB})$. The former experimental observation contradicts the early conjecture that the classical support of the correlation was believed to be equal to or greater than its quantumness for any quantum state [2,3,5,17]. However, such an observation is consistent with previous theoretical predictions [15,66]. It is also interesting to compare the dynamics of the quantum correlation with the relaxation of the system as described in Sec. III C. Note, for example, that the decoherence time of the quantum correlation for the state $|X_{\text{random}}\rangle$ is about 8 ms, the same order of magnitude for the relaxation characteristic times $\tau_T, \tau_{L_1}, \tau_{L_2} \sim 13$ ms. The other initial pseudopure states exhibit similar behavior.

V. CONCLUDING REMARKS

Although entanglement is usually criticized in NMR systems, several quantum protocols have been successfully implemented and have been tested in such a scenario [31,37–39]. The debate about the quantum nature of NMR implementations for QIP [37] is renewed due to the fact that separable states can exhibit nonclassical correlation, which may be responsible for the computational speedup in the NMR context [13]. Therefore, the investigations about such a general correlation in an NMR system become quite relevant.

In this paper, we theoretically and experimentally studied the dynamics of bipartite quantum and classical correlations in an NMR quadrupolar system under the action of the decoherence process (mainly caused by the EFG fluctuations). We reported the observation of a nonclassical correlation in an effective two-qubit NMR system. We also provided an approach for computing the quantum and classical correlations in such a composed system from the experimentally accessible NMR deviation-density matrix.

We have found that classical and quantum correlations decay monotonically in time, by following an exponential law, which is in perfect agreement with the behavior predicted by the theoretical model that was presented. By depending on the initial state (random or Bell-basis pseudopure states), the relation between the amount of quantum and classical correlations changes. Our results show that the nonclassical correlation can be generated and can be manipulated in spin-pseudopure states of NMR systems at room temperature. In our experiments, the quantum aspect of correlation decays monotonically within the longitudinal and transverse relaxation characteristic times. Although the experimental realizations were performed in a specific quadrupolar NMR system, the methods developed here are quite general and can readily be applied to other NMR systems or whichever system uses a deviation-density matrix formalism. It is worth mentioning that, despite the fact that we prepared specific pseudopure states used in the context of the NMR QIP, the results are valid for any initial NMR state concerning its specific $\Delta\rho$. In other words, initial states obtained after simpler excitation schemes without temporal or spatial averaging may also have nonclassical correlations that show similar behavior. The results presented here may shed new light on the quantum resources available in the NMR scenario for QIP implementations.

ACKNOWLEDGMENTS

We acknowledge financial support from the Brazilian funding agencies CAPES, CNPq, and FAPESP. J.M. and L.C.C. are also grateful to UFABC. This work was performed as part of the Brazilian National Institute for Science and Technology of Quantum Information (INCT-IQ).

[1] H. Ollivier and W. H. Zurek, Phys. Rev. Lett. **88**, 017901 (2001).
[2] L. Henderson and V. Vedral, J. Phys. A **34**, 6899 (2001).
[3] V. Vedral, Phys. Rev. Lett. **90**, 050401 (2003).
[4] J. Oppenheim, M. Horodecki, P. Horodecki, and R. Horodecki, Phys. Rev. Lett. **89**, 180402 (2002).
[5] B. Groisman, S. Popescu, and A. Winter, Phys. Rev. A **72**, 032317 (2005).
[6] S. Luo, Phys. Rev. A **77**, 022301 (2008).
[7] K. Modi, T. Paterek, W. Son, V. Vedral, and M. Williamson, Phys. Rev. Lett. **104**, 080501 (2010).
[8] B. M. Terhal, M. Horodecki, D. W. Leung, and D. P. DiVincenzo, J. Math. Phys. (NY) **43**, 4286 (2002).
[9] D. P. DiVincenzo, M. Horodecki, D. W. Leung, J. A. Smolin, and B. M. Terhal, Phys. Rev. Lett. **92**, 067902 (2004).
[10] A. Ferraro, L. Aolita, D. Cavalcanti, F. M. Cucchietti, and A. Acin, Phys. Rev. A **81**, 052318 (2010).
[11] A. Datta, A. Shaji, and C. M. Caves, Phys. Rev. Lett. **100**, 050502 (2008).
[12] B. P. Lanyon, M. Barbieri, M. P. Almeida, and A. G. White, Phys. Rev. Lett. **101**, 200501 (2008).
[13] V. Vedral, e-print arXiv:0906.3656.
[14] L. C. Celeri, A. G. S. Landulfo, R. M. Serra, and G. E. A. Matsas, e-print arXiv:1003.4477 (2010).
[15] J. Maziero, L. C. Céleri, R. M. Serra, and V. Vedral, Phys. Rev. A **80**, 044102 (2009).
[16] W. H. Zurek, Phys. Rev. A **67**, 012320 (2003).
[17] M. Horodecki, P. Horodecki, R. Horodecki, J. Oppenheim, A. Sen, U. Sen, and B. Synak-Radtke, Phys. Rev. A **71**, 062307 (2005).
[18] C. A. Rodríguez-Rosario, K. Modi, A.-m. Kuah, A. Shaji, and E. C. G. Sudarshan, J. Phys. A **41**, 205301 (2008).
[19] M. Piani, P. Horodecki, and R. Horodecki, Phys. Rev. Lett. **100**, 090502 (2008).
[20] A. Shabani and D. A. Lidar, Phys. Rev. Lett. **102**, 100402 (2009).
[21] A. Datta and S. Gharibian, Phys. Rev. A **79**, 042325 (2009).
[22] M. Piani, M. Christandl, C. E. Mora, and P. Horodecki, Phys. Rev. Lett. **102**, 250503 (2009).
[23] T. Werlang, S. Souza, F. F. Fanchini, and C. J. Villas Boas, Phys. Rev. A **80**, 024103 (2009).
[24] F. F. Fanchini, T. Werlang, C. A. Brasil, L. G. E. Arruda, and A. O. Caldeira, Phys. Rev. A **81**, 052107 (2010).
[25] J. Maziero, T. Werlang, F. F. Fanchini, L. C. Céleri, and R. M. Serra, Phys. Rev. A **81**, 022116 (2010).
[26] J. Maziero, L. C. Celeri, and R. M. Serra, e-print arXiv:1004.2082.
[27] J. Maziero, H. C. Guzman, L. C. Céleri, M. S. Sarandy, and R. M. Serra, e-print arXiv:1002.3906.
[28] F. F. Fanchini, L. K. Castelano, and A. O. Caldeira, e-print arXiv:0912.1468.
[29] J.-S. Xu, X.-Y. Xu, C.-F. Li, C.-J. Zhang, X.-B. Zou, and G.-C. Guo, Nat. Commun. **1**, 7 (2010).
[30] E. Knill and R. Laflamme, Phys. Rev. Lett. **81**, 5672 (1998).
[31] I. S. Oliveira, T. J. Bonagamba, R. S. Sarthour, J. C. C. Freitas, and E. R. deAzevedo, *NMR Quantum Information Processing* (Elsevier, Amsterdam, 2007).
[32] J. Stolze and D. Suter, *Quantum Computing: A Short Course from Theory to Experiment*, 2nd ed. (Wiley-VCH, Berlin, 2008).
[33] J.-S. Lee and A. K. Khitrin, J. Chem. Phys. **122**, 041101 (2005).
[34] C. Negrevergne, T. S. Mahesh, C. A. Ryan, M. Ditty, F. Cyr-Racine, W. Power, N. Boulant, T. Havel, D. G. Cory, and R. Laflamme, Phys. Rev. Lett. **96**, 170501 (2006).
[35] D. G. Cory *et al.*, Fortschr. Phys. **48**, 875 (2000).
[36] M. A. Nielsen, E. Knill, and R. Laflamme, Nature (London) **396**, 52 (1998).
[37] R. Laflamme, D. G. Cory, C. Negrevergne, and L. Viola, Quantum Inf. Comput. **2**, 166 (2002).
[38] S. L. Braunstein, C. M. Caves, R. Jozsa, N. Linden, S. Popescu, and R. Schack, Phys. Rev. Lett. **83**, 1054 (1999).
[39] N. Linden and S. Popescu, Phys. Rev. Lett. **87**, 047901 (2001).
[40] A. Abragam, *The Principles of Nuclear Magnetism* (Oxford University Press, New York, 1978).
[41] L. M. K. Vandersypen and I. L. Chuang, Rev. Mod. Phys. **76**, 1037 (2004).
[42] F. A. Bonk, R. S. Sarthour, E. R. deAzevedo, J. D. Bulnes, G. L. Mantovani, J. C. C. Freitas, T. J. Bonagamba, A. P. Guimarães, and I. S. Oliveira, Phys. Rev. A **69**, 042322 (2004).
[43] F. A. Bonk, E. R. deAzevedo, R. S. Sarthour, J. D. Bulnes, J. C. C. Freitas, A. P. Guimarães, I. S. Oliveira, and T. J. Bonagamba, J. Magn. Res. **175**, 226 (2005).
[44] R. R. Ernst, G. Bodenhausen, and A. Wokaun, *Principles of Nuclear Magnetic Resonance in one and two Dimensions* (Oxford University Press, New York, 1990).
[45] A. P. Guimarães, *Magnetism and Magnetic Resonance in Solids* (Wiley Interscience, New York, 1998).
[46] K. S. Slichter, *Principles of Magnetic Resonance*, 3rd ed. (Springer, Berlin, 1990).
[47] J. A. Jones, Prog. Nucl. Magn. Reson. Spectrosc. **38**, 325 (2001).
[48] A. K. Khitrin and B. M. Fung, J. Chem. Phys. **112**, 6963 (2000).
[49] N. Sinha, T. S. Mahesh, K. V. Ramanathan, and A. Kumar, J. Chem. Phys. **114**, 4415 (2001).
[50] A. G. Redfield, IBM J. Res. Dev. **1**, 19 (1957).
[51] H. P. Breuer and F. Petruccione, *The Theory of Open Quantum Systems* (Oxford University Press, New York, 2007); T. C. Stringfellow and T. C. Farrar, Concepts Magn. Reson. **10**, 261 (1998).
[52] T. M. Cover and J. A. Thomas, *Elements of Information Theory* (Wiley Interscience, New York, 2006).

[53] M. A. Nielsen and I. L. Chuang, *Quantum Computation and Quantum Information* (Cambridge University Press, Cambridge, UK, 2000).
[54] G. Benenti, G. Casati, and G. Strini, *Principles of Quantum Computation and Information* (World Scientific, Singapore, 2007), Vol. 2.
[55] V. Vedral, *Introduction to Quantum Information Science* (Oxford University Press, New York, 2006).
[56] B. Schumacher and M. D. Westmoreland, Phys. Rev. A **74**, 042305 (2006).
[57] G. Lipari and A. Szabo, J. Am. Chem. Soc. **104**, 4546 (1982).
[58] G. Jaccard, S. Wimperis, and G. Bohenhausen, J. Chem. Phys. **85**, 6282 (1986).
[59] R. Auccaise, J. Teles, R. S. Sarthour, T. J. Bonagamba, I. S. Oliveira, and E. R. deAzevedo, J. Magn. Res. **192**, 17 (2008).
[60] E. M. Fortunato, M. A. Pravia, N. Boulant, G. Teklemariam, T. F. Havel, and D. G. Cory, J. Chem. Phys. **116**, 7599 (2002).
[61] H. Kampermann and W. S. Veeman, J. Chem. Phys. **122**, 214108 (2005).
[62] J. Teles, E. R. deAzevedo, R. Auccaise, R. S. Sarthour, I. S. Oliveira, and T. J. Bonagamba, J. Chem. Phys. **126**, 154506 (2007).
[63] P. S. Hubbard, J. Chem. Phys. **53**, 985 (1970).
[64] T. E. Bull, J. Magn. Res. **8**, 344 (1972).
[65] K. Radley, L. W. Reeves, and A. S. Tracey, J. Chem. Phys. **80**, 174 (1976).
[66] S. Luo, Phys. Rev. A **77**, 042303 (2008).